

Early warning signals of simulated Amazon rainforest dieback

Chris A. Boulton · Peter Good · Timothy M. Lenton

Received: 12 February 2013 / Accepted: 13 May 2013 / Published online: 29 May 2013
© The Author(s) 2013. This article is published with open access at Springerlink.com

Abstract We test proposed generic tipping point early warning signals in a complex climate model (HadCM3) which simulates future dieback of the Amazon rainforest. The equation governing tree cover in the model suggests that zero and non-zero stable states of tree cover co-exist, and a transcritical bifurcation is approached as productivity declines. Forest dieback is a non-linear change in the non-zero tree cover state, as productivity declines, which should exhibit critical slowing down. We use an ensemble of versions of HadCM3 to test for the corresponding early warning signals. However, on approaching simulated Amazon dieback, expected early warning signals of critical slowing down are not seen in tree cover, vegetation carbon or net primary productivity. The lack of a convincing trend in autocorrelation appears to be a result of the system being forced rapidly and non-linearly. There is a robust rise in variance with time, but this can be explained by increases in inter-annual temperature and precipitation variability that force the forest. This failure of generic early warning indicators led us to seek more system-specific, observable indicators of changing forest stability in the model. The sensitivity of net ecosystem productivity to temperature anomalies (a negative correlation) generally increases as dieback approaches, which is attributable to a non-linear sensitivity of ecosystem respiration to temperature. As a result, the sensitivity of atmospheric CO₂ anomalies to temperature anomalies (a positive correlation) increases as dieback approaches. This stability indicator has the benefit of being readily observable in the real world.

Keywords Amazon dieback · Early warning · Tipping point · HadCM3

Introduction

In recent years, research into the field of tipping points and their predictability has yielded several suggestions for generic early warning signals of an approaching bifurcation-type tipping point (Scheffer et al. 2009; Lenton 2011). The most general behaviour of a dynamical system approaching a bifurcation (where an attractor loses its stability) is that it becomes more sluggish in its recovery from short-term fluctuations (Wissel 1984). This is termed ‘critical slowing down’, and occurs because negative feedback in the system (which keeps it in a given attractor) begins to be overwhelmed by positive feedback (which can propel a transition between attractors)—or more mathematically speaking, the leading eigenvalue governing the decay rate of fluctuations tends toward zero (from a negative value). This critical slowing down behaviour should manifest itself as increasing autocorrelation in time (and possibly space), which can be readily measured. It is also generally expected to cause a rise in variance (Carpenter and Brock 2006), which requires less data to detect a signal. However, there are special conditions under which rising variance does not occur, or cannot be detected (Dakos et al. 2012).

To date, these proposed generic tipping point early warning indicators have been tested in paleo-data approaching past abrupt climate changes (Livina and Lenton 2007; Dakos et al. 2008), and in simple and intermediate complexity climate models approaching forced tipping points (Lenton 2011), but not in the full-complexity models used for climate projections, e.g. by the Intergovernmental Panel on Climate Change. Furthermore, existing model tests of early warning indicators have generally concentrated on the case study of a collapse of the thermohaline circulation of

C. A. Boulton (✉) · T. M. Lenton
College of Life and Environmental Sciences, University of Exeter,
Exeter EX4 4PS, UK
e-mail: c.a.boulton@exeter.ac.uk

P. Good
Met Office Hadley Centre, FitzRoy Road,
Exeter EX1 3PB, UK

the Atlantic, and they have used very slow forcing relative to the rate at which humans are interfering with the climate system (Held and Kleinen 2004).

Here, we set about to test generic early warning indicators of an approaching tipping point in a complex climate model, forced in a realistic way, which exhibits an iconic example of a potential tipping point response to climate change; dieback of the Amazon rainforest. The model we use is the Hadley Centre climate model version 3, known as ‘HadCM3’. Amazon dieback was first predicted when an offline vegetation model was forced with climate change from HadCM3 (and its predecessor HadCM2) (White et al. 1999). Then dieback was found in the fully coupled but lower resolution HadCM3LC model under future forcing (Cox et al. 2000). The equilibrium behaviour of HadCM3LC was later found to have an even stronger non-linear response of Amazon forest cover to temperature (Jones et al. 2009). Unlike reality, 57 different versions of HadCM3 now exist with different settings of key physical model parameters and therefore different climates (Lambert et al. 2013). We show an example of Amazon dieback under future forcing (with the SRES A1B emissions scenario) in one of these model versions in Fig. 1. First, there is a decline in net primary productivity (NPP) (Fig. 1a), then vegetation carbon (Fig. 1b), then broadleaf tree fraction (Fig. 1c), the

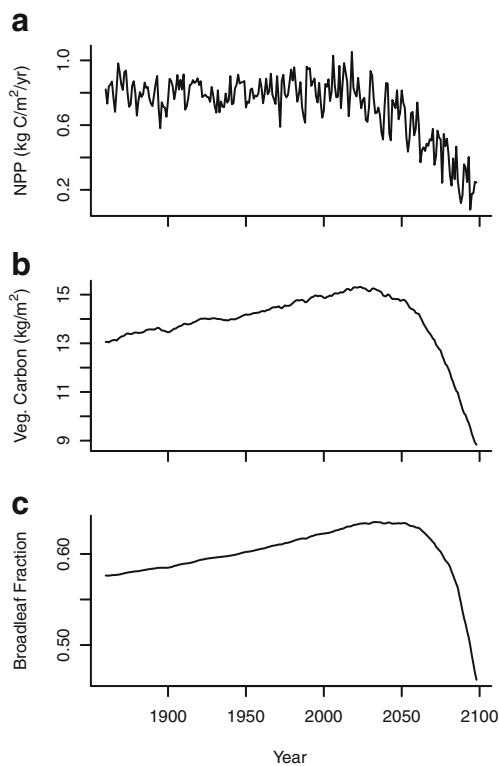


Fig. 1 An example of Amazon dieback simulated in one of the 57 versions of HadCM3 showing the full time series (1860–2100) of **a** net primary productivity (NPP), **b** vegetation carbon and **c** broadleaf fraction, averaged annually over the region

latter beginning around 2060. Below, we make use of all 57 model versions to study multiple realisations of approaching Amazon dieback, and thus begin to examine the statistical reliability of proposed early warning indicators.

Amazon dieback presents an important case study for several reasons. The Amazon rainforest is a critical component of the global carbon cycle, acting as a large store of carbon and typically a significant carbon sink, with the notable exception of recent drought years when it switched to become a carbon source (Phillips et al. 2009; Lewis et al. 2011). The Amazon has been identified as a potential tipping element in the Earth’s climate system (Lenton et al. 2008), partly because alternative attractors for the vegetation–climate system of the region are thought to exist (Oyama and Nobre 2003; Salati and Vose 1984), and partly because in some future simulations, a large fraction of the Amazon dies back fairly abruptly (within decades) (White et al. 1999; Cox et al. 2004; Cook and Vizy 2008). Experts gave an average 20 % chance of tipping the Amazon (at least half of its current area is converted from year-round forest due to climate change) if global warming is between 2 and 4 °C by 2200, and a 70 % chance if warming exceeds 4 °C (Kriegler et al. 2009). However, the future of the Amazon rainforest is highly uncertain. The observational record shows a lengthening of the dry season, attributed to anthropogenic forcing altering the Walker circulation of the atmosphere in the tropics (Vecchi et al. 2006). In HadCM3, this drying trend continues into the future, and together with warming, this overwhelms the tendency of rising atmospheric CO₂ to protect the forest by increasing the efficiency of photosynthesis (Cox et al. 2004). However, future projections with other general circulation models of the climate (GCMs) give very different precipitation trends over the region in the future (Li et al. 2006). Hence, the change in climate and vegetation of the Amazon in HadCM3 is an extreme result among existing models, with a transition to seasonally dry forest in the Eastern Amazon region considered more realistic (Malhi et al. 2009).

Whilst testing generic early warning signals on the Amazon rainforest is new, there have been previous attempts to better understand the Amazon’s vulnerability in terms of observable variables, such as sea surface temperatures (SSTs) in the tropical Pacific (Cox et al. 2004) or the North Atlantic (Cox et al. 2008). The vulnerability of modelled tropical forest cover has been assessed with respect to temperature and dry-season length (DSL) (Good et al. 2011). An approximately linear boundary in the temperature–DSL plane separates forested from un-forested tropical (20° N–20° S) grid cells. This boundary exists in both the HadCM3LC (Good et al. 2011) and HadGEM2-ES (Good et al. 2013) climate models, which both include the Top-down Representation of Interactive Foliage and Flora Including Dynamics (TRIFFID) vegetation model. Looking

across a wider range of models, inter-annual anomalies in atmospheric CO₂ due to anomalies in tropical land carbon storage can be related to anomalies in tropical temperature, due to, e.g. drought or El Niño events (Cox et al. 2013).

For dieback of the Amazon to display tipping point behaviour and corresponding early warning signals, there must be positive feedback in the dynamics of forest loss. Furthermore, for early warning signals to show up in a model study, these positive feedbacks must be captured in the model. A key positive feedback that is (to varying degrees) captured in existing climate models, including HadCM3, is between vegetation and rainfall. Essentially, the forest recycles water to the atmosphere through transpiration and this promotes further precipitation, which supports the forest (Betts 1999; Salati 1987; Salati and Vose 1984). With the prevailing wind travelling inland, this promotes the existence of forest in parts of the Amazon basin farthest from the Atlantic coast. This positive feedback may be strong enough to produce alternative stable states of vegetation cover in parts of the Amazon (Oyama and Nobre 2003). However, such bi-stability is not a necessary condition for the existence of early warning signals (Lenton et al. 2008; Kéfi et al. 2012).

It has not been previously established whether the HadCM3 model exhibits bi-stability of vegetation cover in parts of the Amazon region. We examine the governing equation for tree cover below, which suggests there are two equilibrium solutions even without coupling to the climate. Consistent with this, we find evidence of bi-modality of tree coverage in the full climate model, when looking across different Amazon grid cells (Fig. 2). The state without trees is typically dominated by C3 grasses. The two states could arise purely from the competition dynamics in the vegetation model, but they may be reinforced by vegetation-rainfall feedback. Regardless of

this, even if there was only one equilibrium solution for tree cover in the model, it is already known that Amazon tree cover (averaged across the region) shows a strong non-linear response to temperature (Jones et al. 2009). Furthermore, such a strong non-linear response should mean that generic early warning signals of approaching dieback are present, as long as the model is forced slowly and subject to low amplitude stochastic variability (such that it remains close to its equilibrium behaviour) (Kéfi et al. 2012). A potential caveat here is that the model Amazon system exhibits inertia such that it lags the climate forcing by several decades. This raises the question of whether proposed early warning indicators might reveal the equilibrium (committed) behaviour of the forest rather than the transient (observed) change, or whether they may fail altogether.

Data and methods

HadCM3 Earth system ensemble

Our data was obtained from a ‘perturbed physics’ ensemble of versions of the HadCM3 model called HadCM3-ESE (Earth system ensemble). The ensemble contains 57 members (i.e. model versions) where key parameters have been perturbed within boundaries suggested by experts (Lambert et al. 2013). These parameters are grouped according to their role in the Earth system, whether they are within the atmosphere ($n=32$ parameters) (Collins et al. 2011), ocean ($n=15$) (Collins et al. 2007), sulphur cycle ($n=8$) (Lambert et al. 2013) or carbon cycle ($n=8$) (Booth et al. 2012). Each of the 57 ensemble members contains a combination of changes to these four subsystems, determined by a Latin hypercube sampling process to maximise the spread of atmosphere and carbon cycles used. We are restricted to the data that has already been saved from these existing model runs as it is extremely computationally expensive to rerun the model.

The different ensemble members (i.e. model versions) are all subject to the same forcing scenario spanning 1860–2100, with historical forcing up to 2000 and the Special Report on Emissions Scenarios A1B scenario thereafter (Nakicenovic and Swart 2000). The forcing comprises emissions of carbon dioxide, other greenhouse gases and aerosols, with the model determining their concentrations and the resulting climate effects interactively. A1B can be viewed as a ‘middle of the road’ scenario with an economic rather than an environment focus and a balanced energy usage, as opposed to being fossil fuel intensive for example. The resulting 57 different model runs behave differently thanks to the perturbations to the physics between model versions.

We define the Amazon region in the model as 40–70° W and 15°S–5° N, which comprises 61 land grid cells. In a particular ensemble member, some of these grid cells may

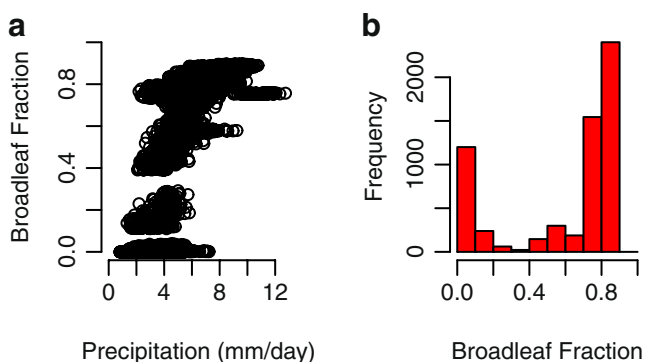


Fig. 2 Bi-modality of tree cover looking across Amazon grid cells in the same version of HadCM3 as in Fig. 1: **a** broadleaf fraction as a function of mean annual precipitation for all Amazon grid cells over the first century of the run (61 points each with 100 years), **b** a histogram of the distribution of tree cover at the grid cell scale when averaging over variations in precipitation

not be forested in 1860, but that allows us to capture forest growth in these regions should it occur later on in the time series. Within a single chosen ensemble member (shown in Figs. 1 and 2), we examined the behaviour of key variables in each of the 61 individual grid cells. When looking across the whole ensemble of model versions, we averaged over this spatial information, on an annually averaged timescale, to produce a single time series for each variable of interest in each of the 57 ensemble members. Comparing the two approaches allowed us to check whether averaging over the whole region affected our results, compared to using grid points individually, noting that the conditions that destabilise the Amazon rainforest are unlikely to be uniform across the region.

Three key output variables from the land surface scheme and the TRIFFID dynamic global vegetation model (Cox 2001) are the focus of our time series analysis: broadleaf fraction (BL), vegetation carbon (VC) and NPP. Two ‘driver’ time series over the Amazon region, temperature and precipitation, are also analysed. In our search for more process-based indicators, we also consider net ecosystem productivity (NEP), by subtracting the soil (heterotrophic) respiration flux from NPP, and atmospheric CO₂ (over the Amazon region), which contains both a long-term, global forcing trend and short-term (inter-annual) variability that reflects changes in NEP of the region.

For each ensemble member, we examined the time series of BL to see if there was a decline (often following a steady rise). If this was seen, we considered the inflection point at which BL starts to decline as the beginning of dieback in the model and only use data up to that point in our main analysis. Across the 57 ensemble members, 31 show dieback starting before 2100. We cannot rule out that dieback will occur later in the other 26 ensemble members, particularly given that committed change of the forest is much greater than transient change in this model. All 57 members are used despite the fact that some models only have small forest coverage, since any amount of forest could exhibit dieback. Models that do not exhibit dieback give time series which are 240 points long, whereas those that exhibit dieback have an average time series of 204 points on which to test for early warning signals.

For the single ensemble member where we consider spatial information, we first determine if there is enough forest in each grid point in the Amazon region to be considered for analysis. If there is a broadleaf fraction less than 0.1 at the start of the time series which does not show any growth, then we ignore this grid point. This leaves 49 (of 61) grid points that contain sufficient forest, and in 43 of these 49 grid points, there is dieback under future forcing. In this case, the average time series length for analysis is approximately 215 points.

Early warning indicators

We use a kernel smoothing function with a bandwidth of 10 years or points (Dakos et al. 2008) to detrend the time series of BL, VC and NPP. Then we use a sliding window length of half the time series (prior to dieback, if it starts) in which we derive AR(1) and variance as potential early warning indicators. We also derive skewness in the same sliding window but from the original rather than the detrended data (Guttal and Jayaprakash 2008). Increasingly positive or increasingly negative skewness can be considered early warning signals because the sign of skewness depends on the position of the attractor being approached. In the analysis of these three time series, we expect to observe skewness becoming more negative over time.

To express trends in the indicators, we use Kendall’s tau rank correlation coefficient (Dakos et al. 2008), which ranges between 1, for an indicator that is always increasing, to -1 for an indicator that is always decreasing. A tau of 0 implies there is no net trend in the indicator and that it increases as much as it decreases.

To provide a null model of the behaviour of these generic indicators under stable boundary conditions, we make use of the control runs of each ensemble member. There were ~70 years of control run available for each member where the forest was stable and no emissions were imposed. We calculate AR(1), variance and skewness on these samples using the methods described above. Then we compare these to the indicator trends observed from a comparable length time series prior to dieback in each model (or the last ~70 years if no dieback occurs).

We also test two process-based, system-specific stability indicators. The first of these assesses how the sensitivity of NEP to temperature anomalies changes over time. The second looks for changes in the sensitivity of atmospheric CO₂ variations of the Amazon region to temperature anomalies. These indicators are motivated by the idea that variations in tropical land carbon storage are caused by tropical temperature anomalies. Respiration is prescribed as an exponential function of temperature whereas photosynthesis is a peaked function of temperature (which allows the possibility that an increase in temperature could cause decreases in photosynthesis if the optimum temperature has been passed). Therefore at higher temperatures, a given increase in temperature should give rise to a greater decrease in NEP and a correspondingly larger addition of CO₂ to the atmosphere.

To calculate these indicators, we detrend the time series of NEP or CO₂ and temperature again using a kernel smoothing function with a bandwidth of 10 years. Then within a sliding window length of 25 years, we estimate the gradient of the best fit (linear regression) line of NEP or CO₂ as a function of temperature, and use the result as an

indicator. We use a smaller window length than in other analyses to better capture the effect of events such as El Niño.

Broadleaf fraction model

We use a simplified version of the TRIFFID model (Cox 2001) to better understand the dynamics:

$$\frac{dV}{dt} = P\hat{V}(1-V) - GV \quad (1)$$

Where V is equal to the broadleaf fraction, G is a disturbance coefficient (0.004/year) and \hat{V} is either the value of V or 0.1 if V falls below 0.1. P is the productivity, in dimensionless area fraction units. There is a non-linear response of the broadleaf fraction (V) to changing productivity (P), with one equilibrium at $V=0$ and another equilibrium solution:

$$V^* = 1 - \frac{G}{P} \quad (2)$$

The equilibrium V^* has an eigenvalue of $G-P$, which is negative for typical values of P found in the ensemble members. As P is reduced, the movement of the equilibrium is non-linear as the eigenvalue approaches zero. Equation

(1) can be rearranged to the normal form of a transcritical bifurcation and it has been confirmed elsewhere that such bifurcations exhibit generic early warning signals (Kuehn 2011). The two stable states observed here should translate into the full GCM version used in the ensemble although complicated due to the calculation of P . The \hat{V} parameter in Eq. (1) prevents the vegetation from becoming negative. However at values of productivity P we use to test the model, this does not alter the fact we are approaching the bifurcation and so should observe early warning signals.

To explore how this model behaves in conditions observed in the full climate model, we ran three 500-member ensembles of the simplified model of tree cover [Eq. (1)]: (1) a ‘null’ model ensemble where there is no forcing on P ($P=0.9$) and a constant noise level ($\sigma=0.003$), (2) a ‘linearly forced’ ensemble where P is reduced linearly from 0.9 to 0.004 (the value of G and hence the transcritical bifurcation point) whilst keeping the same noise level, and (3) a ‘non-linearly forced’ ensemble where P is kept constant for the first 180 years at 0.9 and then reduced linearly from 0.9 to 0.004 over the final 60 years and noise level is increased from $\sigma=0.001$ to $\sigma=0.006$ linearly across the time series to mimic the increase in variance in temperature and precipitation observed in the full model. This third ensemble is an

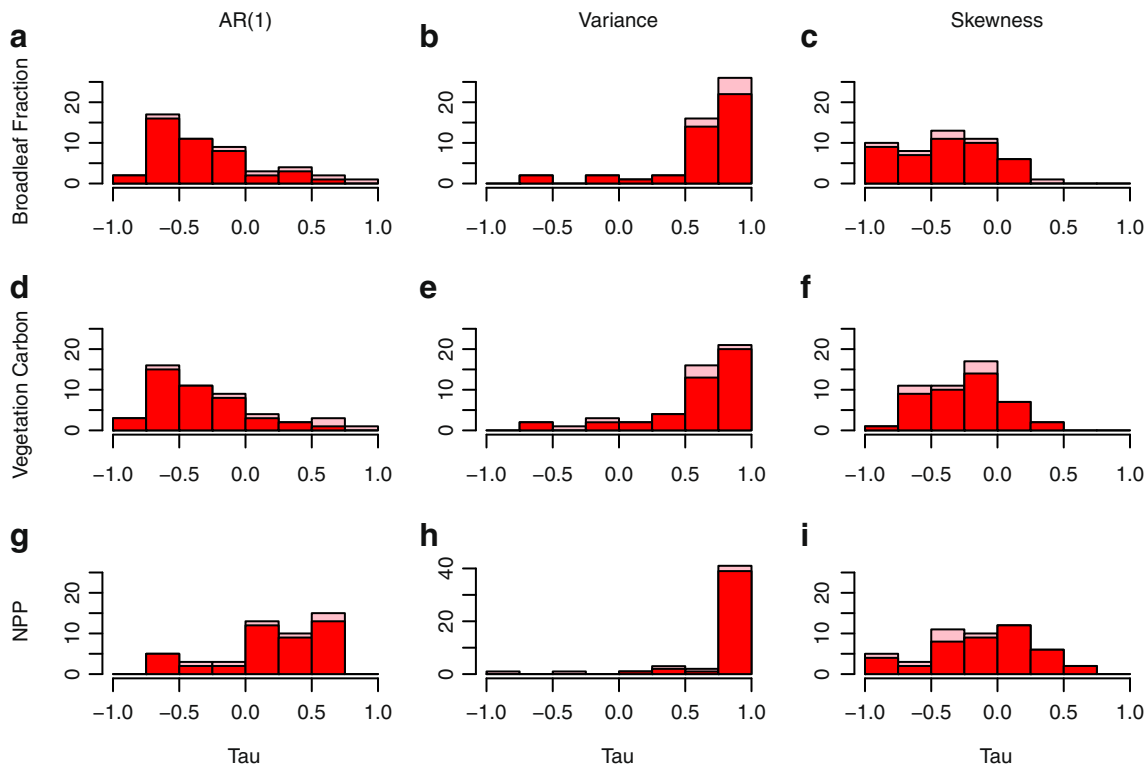


Fig. 3 Trends in generic early warning signals across different grid cells of the version of HadCM3 in Figs. 1 and 2. Annually averaged time series for broadleaf fraction (a–c), vegetation carbon (d–f) and NPP (g–i) are used for each spatial grid point where there is sufficient forest (grid points which have a broadleaf fraction less than 0.1 at the

start of the time series without showing growth are ignored). Note that in **h**, the y-axis has been extended due to the majority of the tau values being in the last bin. In each histogram, the *darker bars* refer to those grid cells which show dieback starting prior to 2100 whereas the (stacked) *lighter bars* are the cells without dieback before 2100

attempt to recreate the conditions seen in the full climate model. In all cases, we analysed the first 200 years of each run, because in cases (2) and (3), dieback never begins before this and generally just after.

Results

HadCM3 Earth system ensemble

In the example model run, dieback starts to occur in the second half of this century around 2060 (Fig. 1). Prior to this, when looking across spatial locations over the first 100 years of the model run, we see evidence of two states for broadleaf tree cover, with one mode around 0.8 and another at 0–0.2 (Fig. 2). When analysing the results from

individual spatial locations within this model run, the majority show dieback, but they do not consistently show the signal of critical slowing down (i.e. rising AR(1) and rising variance) prior to dieback. Typically, there are decreases in AR(1) for broadleaf fraction and vegetation carbon (Fig. 3a, d) and a tendency toward increases in AR(1) for NPP (Fig. 3g). All three variables typically show increases in variance (Fig. 3b, e, h). There are predominantly negative skewness trends observed for broadleaf fraction and vegetation carbon (Fig. 3c, f), but no clear skewness trends for NPP (Fig. 3i).

We analyse the spatially averaged behaviour of this example model run (as in Fig. 1) in Fig. 4. One reason why early warning signals might fail in this and other cases, based on Eq. (1), is that NPP does not start to decline until shortly before dieback begins (where the data is cut off for

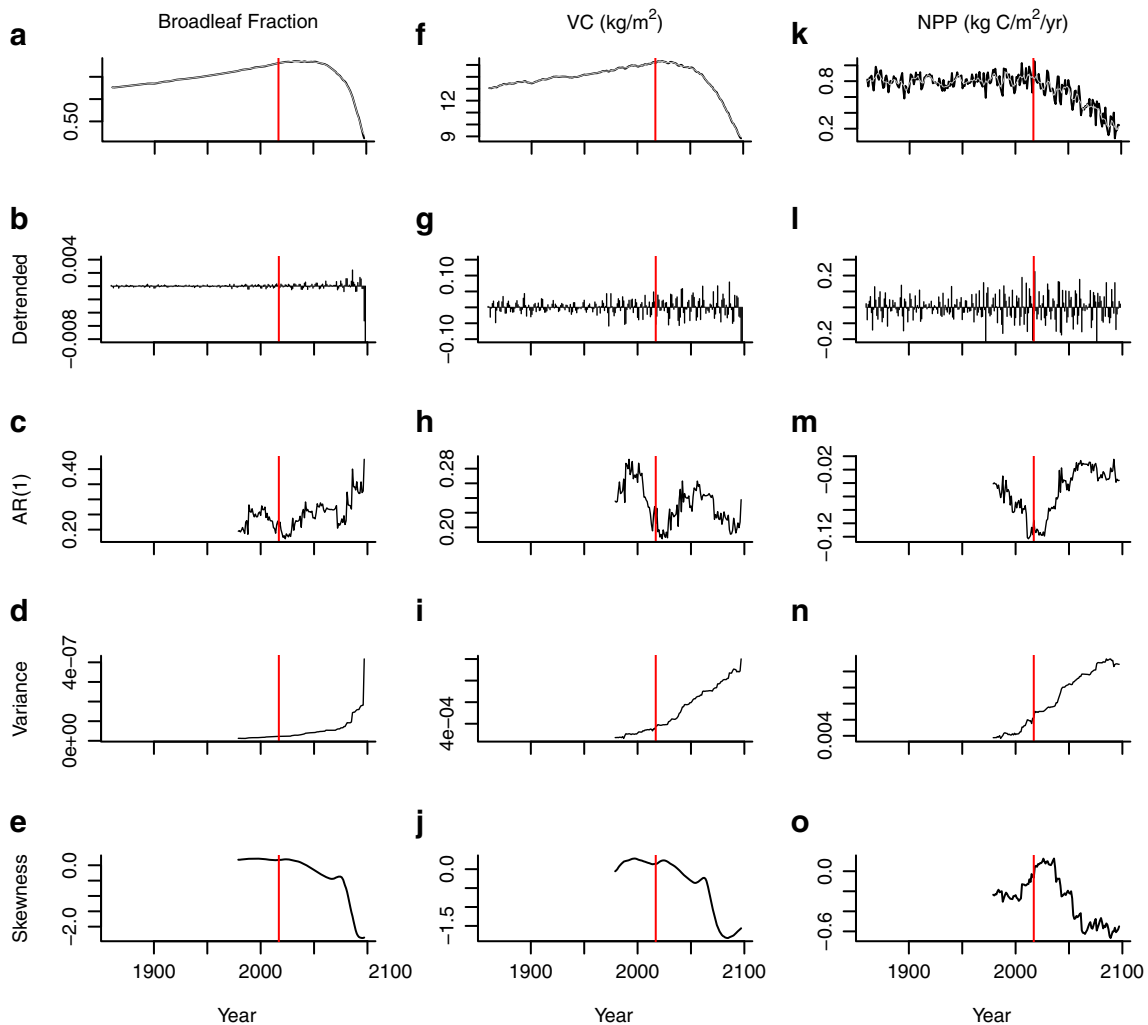


Fig. 4 Early warning signals observed for the three key output variables from the example time series shown in Figs. 1–3. Spatial averages of broadleaf fraction (a–e), vegetation carbon (f–j) and NPP (k–o) are analysed for the full-time series rather than up to observed dieback, in order to examine the full effect of NPP decline that begins around

2020. The start of this decline in productivity is shown in all the time series with a vertical line. The smoothing time series used to derive the residuals (the detrended time series) are shown in the top row (a, f and k) over the original time series

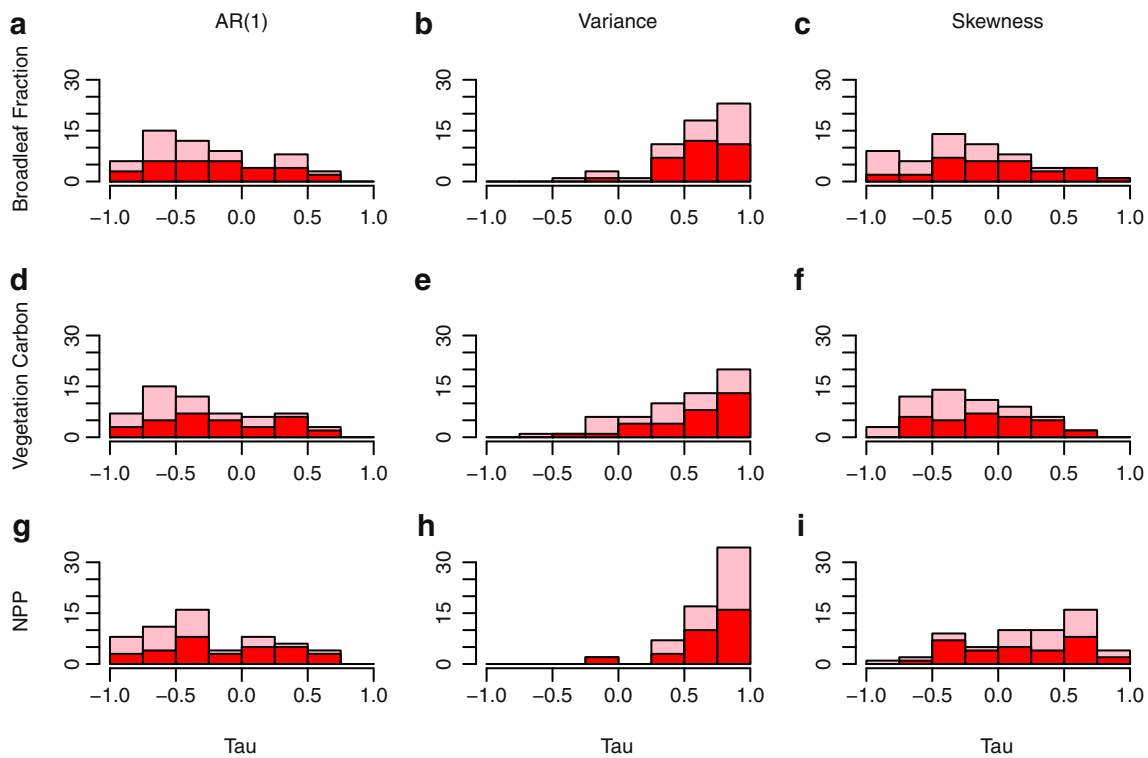


Fig. 5 Trends in proposed generic early warning indicators across the ensemble of 57 models, from analysis of: **a–c** broadleaf fraction, **d–f** vegetation carbon and **g–i** NPP time series averaged over the Amazon region. Trends in AR(1), variance and skewness are expressed as Kendall

tau values. The resulting histograms give an indication of range of indicator trends across the ensemble and their robustness. In each histogram, the *darker bars* refer to those models which show dieback starting prior to 2100 whereas the (stacked) *lighter bars* are the runs without dieback before 2100

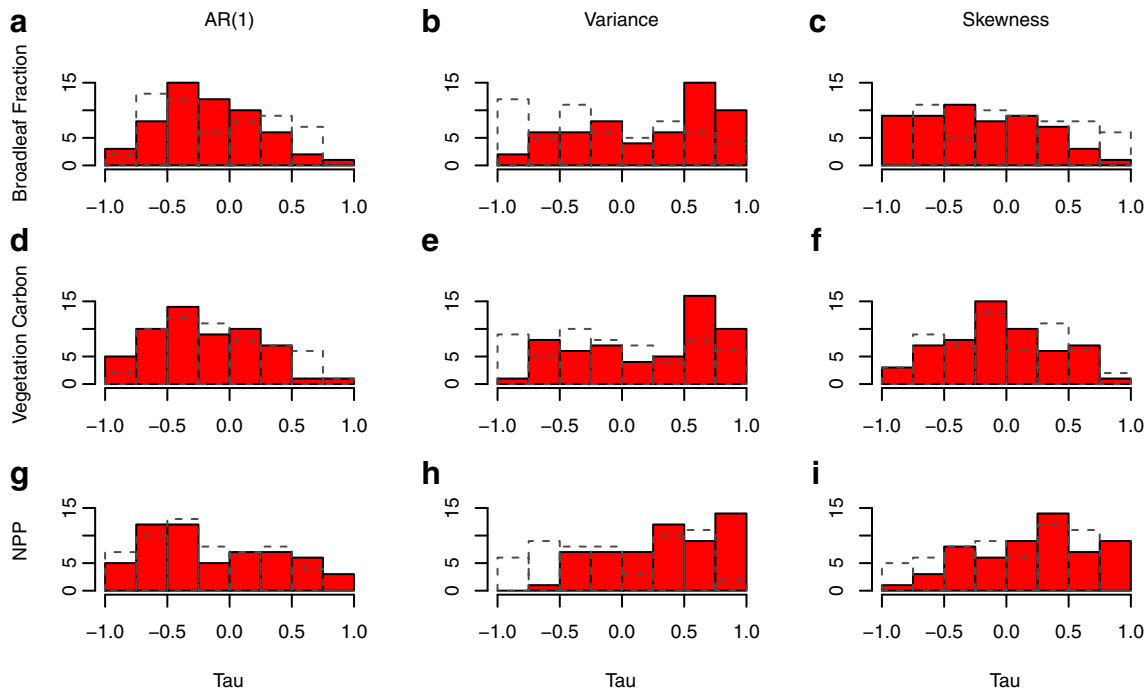


Fig. 6 Trends in generic early warning signals for time series found in control versions of each ensemble member (without forced under an emissions scenario) (*dotted histograms*) compared to the early warning signals found in the original ensemble members using the same length

time series as in the control run time series (~70 years). Broadleaf fraction (**a–c**), vegetation carbon (**d–f**) and NPP (**g–i**) time series were averaged over the Amazon region each year

most of the analyses). Hence in this instance, we analyse the full time series of broadleaf fraction (Fig. 4a, b), vegetation carbon (Fig. 4f, g) and NPP (Fig. 4k, l), showing where NPP begins to decline around 2020 (vertical line in the time series of Fig. 4). Once NPP starts to decline, critical slowing down in tree cover would be expected according to equation [1]. Consistent with this, broadleaf fraction shows a rise in AR(1) and variance and a negative trend in skewness (Fig. 4c, d, e). Vegetation carbon shows an overall decline in AR(1), rise in variance and negative trend in skewness (Fig. 4h, i, j). NPP shows no clear trend in AR(1), rising variance and a trend to negative skewness (Fig. 4m, n, o). However, the encouraging results for broadleaf fraction should be treated with caution as the data set is only one sample of a wide range of signals that the different versions of HadCM3 can produce. Furthermore, in the real world, we are interested in warning signals before dieback begins.

Looking across the ensemble of model versions using spatially averaged data, generic early warning indicators do not show the signal of critical slowing down (i.e. rising AR(1) and rising variance) prior to the start of Amazon dieback. Fig. 5 shows histograms of Kendall tau results for all the ensemble members when testing the AR(1) coefficient, variance and skewness as indicators on the broadleaf fraction, vegetation carbon and NPP time series. AR(1) of broadleaf fraction, vegetation carbon and NPP typically decline, but results with no trend or some increase are also found (Fig. 5a, d, g). The strongest result is rising variance in all three variables (broadleaf fraction, vegetation carbon, NPP) (Fig. 5b, e, h), although occasional downward trends are seen. Broadleaf fraction and vegetation carbon are

typically increasingly negatively skewed over time (Fig. 5c, f), whereas there is a hint of NPP becoming increasingly positively skewed over time (Fig. 5i). In all individual cases examined, there is a switch of sign of skewness of NPP over time. Differences between the results for ensemble members that show Amazon dieback starting before 2100 (dark histograms in Fig. 5) and those that do not (lighter stacked histograms) are modest. There is a slightly stronger tendency of decreasing AR(1) in models with no dieback (Fig. 5a, d, g) and arguably trends in skewness are slightly stronger (Fig. 5c, f, i).

When compared to the control runs where no forcing is imposed on the system, which we are treating as a null model (Fig. 6), the most prominent change in the indicators are an increase in variance in broadleaf fraction, vegetation carbon and NPP (Fig. 6b, e, h). The distribution of trends in AR(1) (Fig. 6a, d and g) and skewness (Fig. 6c, f and i) do not appear significantly different under climate forcing to the control runs of the models. However, we stress here that the time series are short and longer time series would be needed to attempt a statistical test on the significance of the results.

The indicator trend of increasing variance that we do consistently observe could be due to corresponding trends in the environmental variables forcing the forest (Fig. 7). Indeed, we find that temperature generally shows strongly rising variance (Fig. 7b), together with a tendency toward declining AR(1) (Fig. 7a), and perhaps a slight shift to negative skewness (Fig. 7c). Precipitation also tends to show increasing variance or in a smaller number of cases decreasing variance (Fig. 7e), but no clear trend in AR(1) (Fig. 7d) or skewness (Fig. 7f). The increases in variance of temperature and

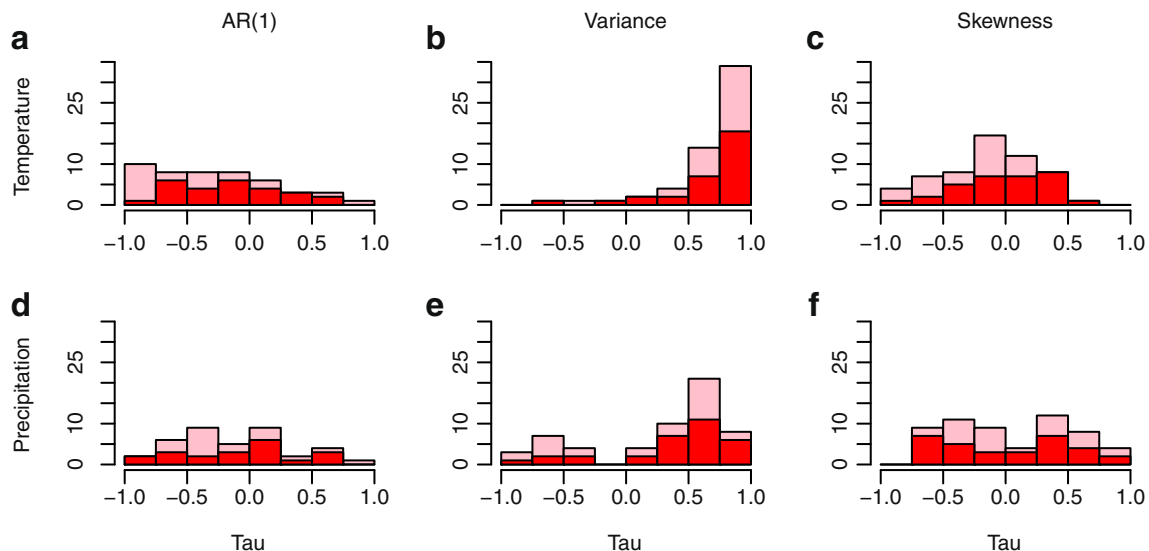


Fig. 7 Trends in the environmental variables of **a–c** temperature and **d–f** precipitation averaged over the Amazon region, across the ensemble of 57 models. Again trends in AR(1) estimation, variance and skewness are

measured as Kendall tau values with the *darker bars* of each histogram referring to ensemble members in which Amazon dieback starts before 2100 and the (stacked) *lighter bars* those in which it does not

precipitation can be mostly attributed to the model producing more frequent or extreme El Niño events under climate forcing, although we should note that temperature and precipitation are not pure external forcing variables—they are also affected by feedback from the forest. We also note that a strong enough increase in variance (as seen for temperature) can cause a decrease in AR(1) because it makes neighbouring points in a time series less alike.

Considering more process-based indicators of forest stability, we find an expected negative correlation between (inter-annual) changes in temperature and (inter-annual) changes in NEP—in other words, warming suppresses NEP (Fig. 8a)—and this explains why CO₂ anomalies are positively correlated with temperature (Fig. 8b)—as carbon is then released from the forest to the atmosphere. These sensitivities generally become stronger with time across the ensemble—which means a negative trend in dNEP/dT (Fig. 8h) and a positive trend in dCO₂/dT (Fig. 8i). In an example run (Fig. 8c–e), the trends in these indicators are

present at least a century before dieback begins (Fig. 8f, g). These results are seen regardless of whether a model shows dieback before 2100 (stacked bars in Fig. 8h, i). Whilst it appears the dCO₂/dT sensitivity shows a slightly more robust increasing tendency in the models that do not exhibit dieback by 2100, a Mann–Whitney *U* test reveals that the two distributions are not statistically significantly different at 5 % significance (*p*=0.066).

Broadleaf fraction model

On examining the behaviour of the simplified model of broadleaf fraction, the null model ensemble produces no significant early warning signals as expected (Fig. 9a–c). In the linearly forced model ensemble, we do find the expected early warning signal of increasing AR(1), together with a slight tendency toward increasing variance, and a tendency toward negative skewness (Fig. 9d–f). However, in the non-linearly forced ensemble, the early warning

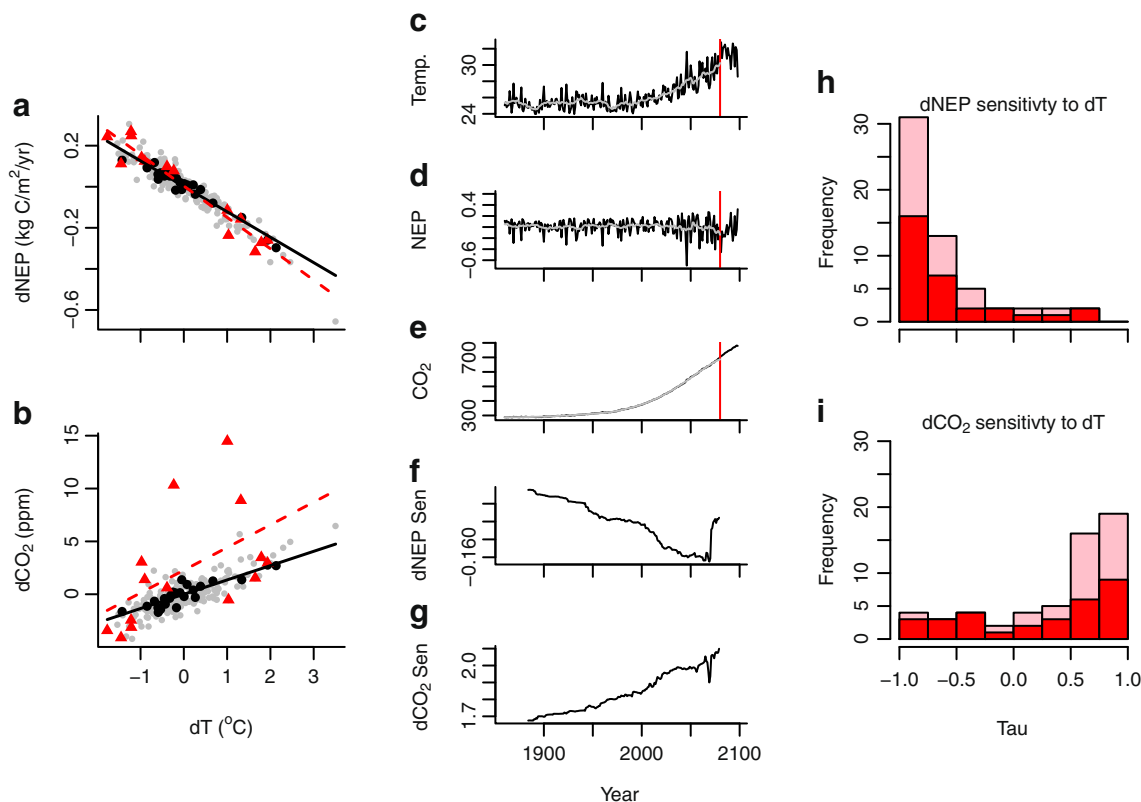


Fig. 8 Changes in the sensitivity of NEP and CO₂ to temperature anomalies over time as early warning indicators: (a–g) shows results for an individual ensemble member, (h,i) summarises results across the ensemble. In a and b, temperature anomalies (dT) are plotted against a NEP (dNEP) and b CO₂ (dCO₂) anomalies, after detrending the time series with bandwidth=10. Using a window length of 25 years, the first window’s points are shown as dark circles and the last using triangles with the corresponding linear regression lines plotted using a solid line and dotted line respectively. The original time series of temperature (in degrees Celsius) (c), NEP (in kilograms of carbon per square metre per

year) (d) and atmospheric CO₂ (in ppm) (e) are shown along with the detrended time series (lighter colour). Only using data prior to the start of dieback in broadleaf fraction (shown by the vertical line in c–e), the gradient of the regression lines for both f dNEP/dT and g dCO₂/dT in sliding windows of 25 years are plotted. Observing the whole ensemble, histograms show the Kendall tau of the resulting trends in sensitivity of h dNEP/dT and i dCO₂/dT. In both cases, the darker bars of each histogram refer to ensemble members that show dieback starting by 2100 whereas the (stacked) lighter bars to not

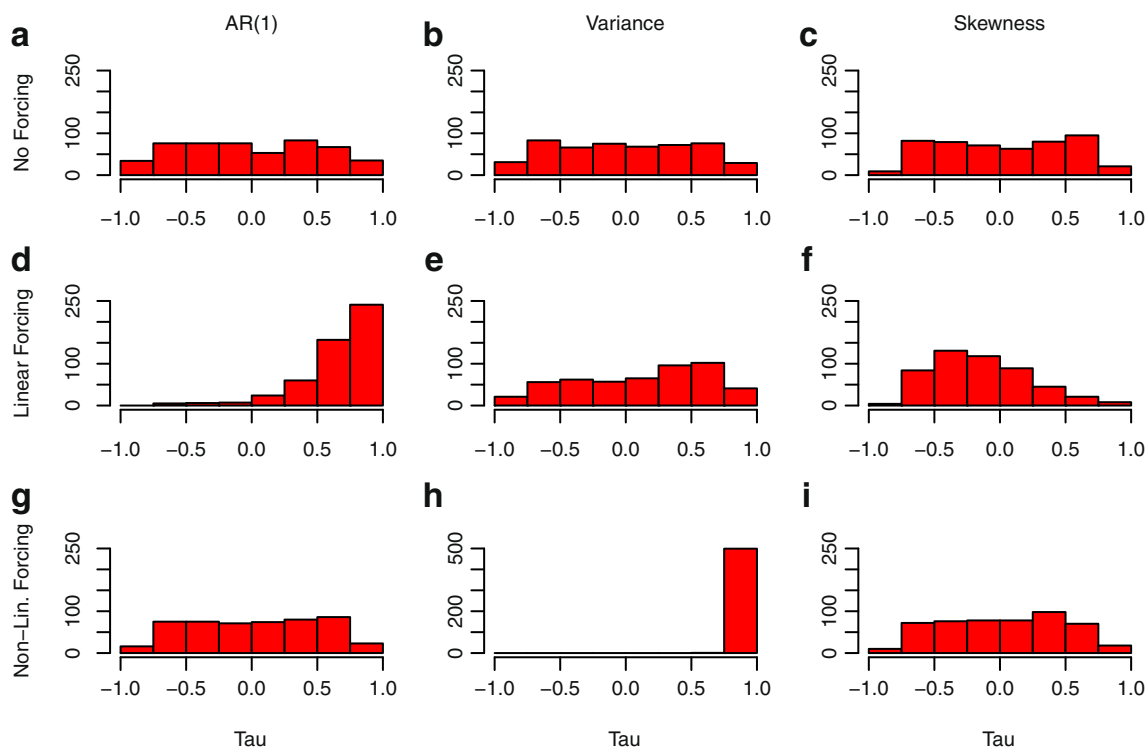


Fig. 9 Results using a simplified version of the governing TRIFFID equation used in HadCM3 to determine broadleaf fraction (Eq. 1). Kendall tau values from early warning signals for the three 500

member ensembles with no forcing (a–c), linear forcing (d–f) and non-linear forcing (g–i) are shown as histograms. Full details on each of the three ensembles are given in the main text

signal from AR(1) is eliminated (with no clear trends in this indicator), whereas variance is strongly increasing reflecting increasing amplitude of the forcing noise, and there are no clear trends in skewness (Fig. 9g–i). These results suggest that the fairly rapid and non-linear forcing of the full climate model may be responsible for eliminating the expected early warning signal of rising autocorrelation.

Discussion

We have analysed time series of the Amazon rainforest in an ensemble of versions of the HadCM3 model, to test both generic and system-specific indicators of an approaching tipping point. Despite Amazon dieback beginning in over half of the ensemble members before 2100, the expected generic early warning signals of an approaching bifurcation-type tipping point are not consistently present. In particular, the expected signal of increasing autocorrelation is missing. There is a robust increase in variance in the models but this may be attributed to increasing variance in key forcing factors for the forest, notably increasing temperature variability driven by El Niño.

The failure to observe generic early warning signals could occur for several reasons. The simplest would be if there was no ‘critical transition’ in the model world. However, we have

several reasons to believe that the model is capable of displaying critical slowing down. As already noted, the equilibrium response of Amazon forest cover to temperature is strongly non-linear (Jones et al. 2009), and such responses should show early warnings signals even if there is no bifurcation (Kéfi et al. 2012). Furthermore, the underlying equations suggest that as NPP declines, and with it forest cover, a transcritical bifurcation is approached. Although the system is a long way from the bifurcation when NPP starts to decline and then dieback begins, it is moving towards the bifurcation and therefore the corresponding leading eigenvalue is increasing toward zero, which should produce critical slowing down. Hence, the explanation for the lack of early warning signals could be that the conditions for observing them—namely that the model is forced slowly and subject to low amplitude, additive stochastic variability (such that it remains close to its equilibrium behaviour)—are violated. Indeed, the full climate model is subject to fairly rapid and non-linear forcing, and when we impose such a forcing in a simplified model of broadleaf fraction, the expected early warning signal of rising autocorrelation is eliminated.

It is also worth noting that we are able to measure generic early warning indicators in our ensemble with relative ease compared to the real world. Observations of time series would be hard to obtain, especially to the degree of accuracy we would need to test, for example, increases in variance in

broadleaf fraction. In this case, observational error would be larger than the measures of variance we generally observe in the time series derived from the models runs.

One critical feedback that is missing from the models analysed here and could contribute to the presence of early warning signals in reality is a positive feedback between vegetation state and fire. Essentially, the presence of trees suppresses fire encouraging their dominance over grasses, whereas the presence of grasses promotes fire, preventing the establishment of trees. This local scale feedback could be responsible for creating alternative attractor states (forest or savannah) across large parts of the Amazon today (Hirota et al. 2011; Staver et al. 2011). Analysis of satellite vegetation cover data suggests a range of precipitation for which forest and savannah states are both stable in the Amazon region, with the forest becoming less 'resilient' (i.e. the basin of attraction becomes shallower) as precipitation declines toward a critical threshold around 1,800 mm/year (or 5 mm/day) (Hirota et al. 2011; Staver et al. 2011). Corresponding spatial locations where there is predicted to be forest-savannah bi-stability are in the southern or south-eastern Amazon, particularly in Bolivia (Hirota et al. 2011). There are also areas of currently low tree cover in south Brazil that are predicted to be bi-stable (Staver et al. 2011). In recent drought years, a critical transition to a 'mega fire' regime has been observed in a part of the Amazon (Pueyo et al. 2010).

Failures of the generic early warning indicators caused us to seek more process-based indicators of changing forest stability in the model. The sensitivity of NEP to temperature anomalies (a negative correlation) generally increases over time (as dieback approaches). This is readily understood because respiration is prescribed as an exponential function of temperature whereas photosynthesis is a peaked function of temperature (and may even switch regime from rising to declining with temperature). Thus, at higher temperatures a given increase in temperature gives rise to a larger decrease in NEP. Furthermore, the sensitivity of atmospheric CO₂ anomalies over the Amazon region to temperature anomalies (a positive correlation) increases robustly, and both of these quantities are readily observable in the real world. The GOSAT satellite record of regional atmospheric CO₂ measurements (including the Amazon region) only began around 2009. However, global CO₂ anomalies are dominated by variability in tropical land carbon stores and they have been measured for longer.

Although these process-based stability indicators are potentially observable, they can only indicate a tendency of changing resilience of the forest (in this case decreasing). There is no particular, universal threshold value which signals Amazon dieback in the model, perhaps because the physics of each model version is different. For example, the forest of one model version may be resilient to dNEP/dT sensitivity (gradient) of -3 , whereas another may show

dieback before this sensitivity is reached. This lack of an absolute indicator of a dieback threshold is also true for generic indicators such as rising variance.

As yet we have not tested any spatial early warning indicators on the data, for example, rising spatial correlation (Dakos et al. 2011; Bathiany et al. 2013). However, the ensemble members in HadCM3-ESE generally show dieback which begins in the north-east of the region and moves towards the centre. In other words, dieback does not occur coherently and simultaneously across the whole region in the model. Hence spatial indicators may fail. Also, we have not performed a grid point by grid point analysis for all the ensemble members, because this would involve individually examining ~3,500 time series. We believe such analysis would be redundant because it is already clear from our analysis of the broadleaf fraction model that due to fast, non-linear forcing of the system, including increasing variance in the driving time series, generic early warning signals—notably rising autocorrelation—tend to fail.

The absence of generic early warning signals of Amazon dieback in the HadCM3 model does not imply they would be absent in the real world. In particular, observational data suggests that there is bi-stability of tree cover at a much finer spatial scale than the model resolves, and this may be due to positive feedbacks between vegetation cover and fire that are not included in HadCM3 (Hirota et al. 2011; Staver et al. 2011). Therefore further research should consider if this can give rise to early warning signals at a finer spatial scale.

Acknowledgments We thank Ben B. Booth for comments and help in obtaining the data, Peter M. Cox for suggestions and Vasilis Dakos and two anonymous reviewers for their constructive feedback. CAB was supported by a PhD studentship funded by the University of Exeter. PG was supported by the Joint DECC/Defra Met Office Hadley Centre Climate Programme (GA01101). TML was supported by the NERC project 'Detecting and classifying bifurcations in the climate system' (NE/F005474/1).

Open Access This article is distributed under the terms of the Creative Commons Attribution License which permits any use, distribution, and reproduction in any medium, provided the original author(s) and the source are credited.

References

- Bathiany S, Claussen M, Fraedrich K (2013) Detecting hotspots of atmosphere-vegetation interaction via slowing down—part 1: a stochastic approach. *Earth Syst Dynam* 4(1):63–78. doi:10.5194/esd-4-63-2013
- Betts RA (1999) Self-beneficial effects of vegetation on climate in an ocean-atmosphere general circulation model. *Geophys Res Lett* 26(10):1457–1460
- Booth BBB, Jones CD, Collins M, Totterdell IJ, Cox PM, Sitch S, Huntingford C, Betts RA, Harris GR, Lloyd J (2012) High sensitivity of future global warming to land carbon cycle processes. *Environ Res Lett* 7(2):024002

- Carpenter SR, Brock WA (2006) Rising variance: a leading indicator of ecological transition. *Ecol Lett* 9(3):311–318. doi:10.1111/j.1461-0248.2005.00877.x
- Collins M, Booth BBB, Bhaskaran B, Harris GR, Murphy JM, Sexton DMH, Webb MJ (2011) Climate model errors, feedbacks and forcings: a comparison of perturbed physics and multi-model ensembles. *Climate Dynam* 36(9–10):1737–1766. doi:10.1007/s00382-010-0808-0
- Collins M, Brierley CM, MacVean M, Booth BBB, Harris GR (2007) The sensitivity of the rate of transient climate change to ocean physics perturbations. *J Climate* 20(10):2315–2320. doi:10.1175/jcli4116.1
- Cook KH, Vizy EK (2008) Effects of twenty-first-century climate change on the Amazon rain forest. *J Climate* 21:542–560
- Cox PM (2001) Description of the “TRIFFID” Dynamic Global Vegetation Model vol Technical Note 24. Hadley Centre
- Cox PM, Betts RA, Collins M, Harris PP, Huntingford C, Jones CD (2004) Amazonian forest dieback under climate-carbon cycle projections for the 21st century. *Theor Appl Climatol* 78:137–156
- Cox PM, Betts RA, Jones CD, Spall SA, Totterdell IJ (2000) Acceleration of global warming due to carbon-cycle feedbacks in a coupled climate model. *Nature* 408:184–187
- Cox PM, Booth BBB, Friedlingstein P, Huntingford C, Jones CD, Pearson D (2013) Interannual variability in carbon dioxide constrains the risk of tropical forest dieback. *Nature* (in press)
- Cox PM, Harris PP, Huntingford C, Betts RA, Collins M, Jones CD, Jupp TE, Marengo JA, Nobre CA (2008) Increasing risk of Amazonian drought due to decreasing aerosol pollution. *Nature* 453:212–215
- Dakos V, Kefi S, Rietkerk M, Nes EH, Scheffer M (2011) Slowing down in spatially patterned ecosystems at the brink of collapse. *American Naturalist* 177:E153–E166. doi:10.1086/659945
- Dakos V, Scheffer M, van Nes EH, Brovkin V, Petoukhov V, Held H (2008) Slowing down as an early warning signal for abrupt climate change. *PNAS* 105(38):14308–14312
- Dakos V, van Nes EH, D’Odorico P, Scheffer M (2012) Robustness of variance and autocorrelation as indicators of critical slowing down. *Ecology* 93:264–271. doi:10.1890/11-0889.1
- Good P, Jones CD, Lowe J, Betts RA, Booth BBB, Huntingford C (2011) Quantifying environmental drivers of future tropical forest extent. *J Climate* 24:1337–1349
- Good P, Jones CD, Lowe J, Betts RA, Gedney N (2013) Comparing tropical forest projections from two generations of Hadley Centre Earth System models, HadGEM2-ES and HadCM3LC. *J Climate* 26(2):495–511. doi:10.1175/jcli-d-11-00366.1
- Guttal V, Jayaprakash C (2008) Changing skewness: an early warning signal of regime shifts in ecosystems. *Ecol Lett* 11:450–460
- Held H, Kleinen T (2004) Detection of climate system bifurcations by degenerate fingerprinting. *Geophys Res Lett* 31, L23207. doi:10.1029/2004GL020972
- Hirota M, Holmgren M, Van Nes EH, Scheffer M (2011) Global resilience of tropical forest and savanna to critical transitions. *Science* 334(6053):232–235. doi:10.1126/science.1210657
- Jones C, Lowe J, Liddicoat S, Betts R (2009) Committed ecosystem change due to climate change. *Nat Geosci* 2:484–487
- Kéfi S, Dakos V, Scheffer M, Van Nes EH, Rietkerk M (2012) Early warning signals also precede non-catastrophic transitions. *Oikos*. doi:10.1111/j.1600-0706.2012.20838.x
- Kriegler E, Hall JW, Held H, Dawson R, Schellnhuber HJ (2009) Imprecise probability assessment of tipping points in the climate system. *PNAS* 106(13):5041–5046
- Kuehn C (2011) A mathematical framework for critical transitions: bifurcations, fast-slow systems and stochastic dynamics. *Physica D: Nonlinear Phenomena* 210(106):1–20
- Lambert FH, Harris G, Collins M, Murphy J, Sexton DH, Booth BB (2013) Interactions between perturbations to different Earth system components simulated by a fully-coupled climate model. *Climate Dynamics*. doi:10.1007/s00382-012-1618-3, pp. 1–18
- Lenton TM (2011) Early warning of climate tipping points. *Nature Climate Change* 1:201–209. doi:10.1038/nclimate1143
- Lenton TM, Held H, Kriegler E, Hall J, Lucht W, Rahmstorf S, Schellnhuber HJ (2008) Tipping elements in the Earth’s climate system. *PNAS* 105(6):1786–1793. doi:10.1073/pnas.0705414105
- Lewis SL, Brando PM, Phillips OL, van der Heijden GMF, Nepstad D (2011) The 2010 Amazon drought. *Science* 331(6017):554. doi:10.1126/science.1200807
- Li W, Fu R, Dickinson RE (2006) Rainfall and its seasonality over the Amazon in the 21st century as assessed by the coupled models for the IPCC AR4. *J Geophys Res* 111, D02111. doi:10.1029/2005JD006355
- Livina VN, Lenton TM (2007) A modified method for detecting incipient bifurcations in a dynamical system. *Geophys Res Lett* 34, L03712. doi:10.1029/2006GL028672
- Malhi Y, Aragao LEOC, Galbraith D, Huntingford C, Fisher R, Zelazowski P, Sitch S, Meece Sweeney C, Meir P (2009) Exploring the likelihood and mechanism of a climate-change-induced dieback of the Amazon rainforest. *Proceedings of the National Academy of Sciences USA* 106:20610–20615
- Nakicenovic N, Swart R (2000) IPCC special report on emissions scenarios. Cambridge University Press, Cambridge
- Oyama MD, Nobre CA (2003) A new climate-vegetation equilibrium state for Tropical South America. *Geophys Res Lett* 30(23):2199
- Phillips OL, Aragao LEOC, Lewis SL, Fisher JB, Lloyd J, Lopez-Gonzalez G, Malhi Y, Monteagudo A, Peacock J, Quesada CA, van der Heijden G, Almeida S, Amaral I, Arroyo L, Aymard G, Baker TR, Banki O, Blanc L, Bonal D, Brando P, Chave J, de Oliveira ACA, Cardozo ND, Czimczik CI, Feldpausch TR, Freitas MA, Gloor E, Higuchi N, Jimenez E, Lloyd G, Meir P, Mendoza C, Morel A, Neill DA, Nepstad D, Patino S, Penuela MC, Prieto A, Ramirez F, Schwarz M, Silva J, Silveira M, Thomas AS, Ht S, Stropp J, Vasquez R, Zelazowski P, Davila EA, Andelman S, Andrade A, Chao K-J, Erwin T, Di Fiore A, Coronado EH, Keeling H, Killeen TJ, Laurance WF, Cruz AP, Pitman NCA, Vargas PN, Ramirez-Angulo H, Rudas A, Salamao R, Silva N, Terborgh J, Torres-Lezama A (2009) Drought sensitivity of the Amazon rainforest. *Science* 323(5919):1344–1347. doi:10.1126/science.1164033
- Pueyo S, De Alencastro Graça PML, Barbosa RI, Cots R, Cardona E, Fearnside PM (2010) Testing for criticality in ecosystem dynamics: the case of Amazonian rainforest and savanna fire. *Ecol Lett* 13(7):793–802. doi:10.1111/j.1461-0248.2010.01497.x
- Salati E (1987) The forest and the hydrological cycle. In: Dickinson RE (ed) *The Geophysiology of Amazonia: vegetation and climate interactions*. Wiley, New York, pp 273–296
- Salati E, Vose PB (1984) Amazon basin: a system in equilibrium. *Science* 225(4658):129–138
- Scheffer M, Bacompte J, Brock WA, Brovkin V, Carpenter SR, Dakos V, Held H, van Nes EH, Rietkerk M, Sugihara G (2009) Early warning signals for critical transitions. *Nature* 461:53–59
- Staver AC, Archibald S, Levin SA (2011) The global extent and determinants of savanna and forest as alternative biome states. *Science* 334(6053):230–232. doi:10.1126/science.1210465
- Vecchi GA, Soden BJ, Wittenberg AT, Held IM, Leetmaa A, Harrison MJ (2006) Weakening of tropical Pacific atmospheric circulation due to anthropogenic forcing. *Nature* 441:73–76
- White A, Cannell MGR, Friend AD (1999) Climate change impacts on ecosystems and the terrestrial carbon sink: a new assessment. *Glob Environ Chang* 9:S21–S30
- Wissel C (1984) A universal law of the characteristic return time near thresholds. *Oecologia* 65(1):101–107. doi:10.1007/bf00384470